SJST
sjst.scst.edu.ly

Surman Journal for Science and Technology
ISSN: Online (2790-5721) - Print (2790-5713)

مجلة صرمان للعلوم والتقنية
Vol 8, No.1. Jan – May. 2026
Pages: 322 ~ 334

Temperature Concentration Optimization of Al_2O_3 Nanoparticles for Enhance Oil Recovery A Process Engineering and Techno-Economic Analysis

Mohamed Lahrash[*1], Elsadeq Elaswod[2]

Petroleum Engineering Department, Faculty of Natural Resources Engineering Bir Elghanam, University of Zawia, Azzawia, Libya

M.lahrash@zu.edu.ly[1], sadiq.85ly@gmail.com[2]

Abstract

This study investigates the influence of temperature and Al_2O_3 nanoparticles concentration on Enhance oil recovery from Libyan sandstone core samples from an industrial engineering lens. A controlled laboratory experiment was executed using three nanoparticles' concentrations (0.0, 0.6 and 1.2g/100ml) and five temperature levels ranged from 30°C to 70°C within a randomized 3X5 full factorial design with each treatment evaluated once at N=15 total runs. Results demonstrate a consistent improvement in recovery factor with increasing in temperature and Al_2O_3 nanoparticles dosage. Baseline waterflooding achieved recovery values between 33% and 41% whereas the introduction of Al_2O_3 nanofluids increased ultimate recovery to a range of 42% to 68%, confirming significant displacement enhancement. Response surface methodology regression analysis demonstrate a highly significant overall model of ($F=60.82$, $df=10$, $p<0.001$) with a significant concentration temperature interaction ($P=0.0085$) A second order response surface model (RSM) was developed to quantify these effect achieving high predictive accuracy (R^2=0.9605, Adjusted $R^2 = 0.9447$, $F = 60.82$, $p = 5.57 \times 10^{-7}$).Findings confirms that Al_2O_3 assisted enhance oil recovery is highly effective for moderate temperature sandstone reservoirs, establishing an empirical basis for operational control and Techno-economic optimization.

Keywords: Process Optimization, Enhanced Oil Recovery, Aluminum Oxide Nanoparticles, Parametric Analysis, Industrial Engineering, Response Surface Methodology

الملخص

تستهدف هذه الدراسة تقييم التأثير المزدوج لكل من درجة الحرارة وتركيز جسيمات أكسيد الألومنيوم النانوية (Al_2O_3) على تحسين استخلاص النفط في المكامن الرملية عبر منظور الهندسة الصناعية وتحسين العمليات. تم تنفيذ تجربة معملية محكمة باستخدام ثلاثة تراكيز من الجسيمات النانوية (0.0، 0.6، و1.2 جم/100 مل) وخمسة مستويات لدرجات الحرارة تتراوح بين 30 و70 درجة مئوية، وذلك ضمن تصميم التحليل العاملي الكامل (3 × 5) بـ 15 تجربة فعلية (N = 15). أظهرت النتائج تحسناً مستمراً في معامل الاستخلاص بزيادة درجة الحرارة وجرعة الجسيمات النانوية. حيث حقق الغمر المائي الأساسي معدلات استخلاص تراوحت بين 33% و41%، في حين أدت الموائع النانوية القائمة على جسيمات Al_2O_3 إلى رفع نسبة الاستخلاص إلى نطاق يتراوح بين 42% و68%، مما يؤكد حدوث تعزيز كبير في كفاءة الإزاحة. أثبت تحليل الانحدار باستخدام منهجية سطح الاستجابة (RSM) وجود نموذج ذي دلالة إحصائية عالية، مع تفاعل حراري-كيميائي جوهري بين التركيز ودرجة الحرارة. كما تم تطوير نموذج رياضي من الدرجة الثانية لتقييم هذه التأثيرات، والذي حقق دقة تنبؤية عالية ($R^2 = 0.9605$). وتؤكد النتائج أن الاستخلاص المعزز للنفط بمساعدة جسيمات Al_2O_3 ذو فعالية عالية للمكامن الرملية ذات الحرارة المعتدلة، مما يؤسس قاعدة تجريبية متينة للتحكم العملياتي والتحليل التقني-الاقتصادي.

Submitted: *06/04/2026* ***Accepted****: 27/05/2026*

1. Introduction

The global energy landscape is defined by increasing demand coupled with declining production from mature oil reservoirs. According to the international energy agency, approximately 80% of

global oil production originates from fields that have already passed peak production capacity, experiencing an average post-peak decline rate of 5.6% a year conventional reserve (Mondal et al., 2026). following primary and secondary recovery over two-thirds of original oil in place OOIP remains trapped and reservoir formation due to high interfacial tension, poor sweep efficiency and reservoir heterogeneity (Mondal et al., 2026).

From an industrial engineering perspective this represents a classic system optimization problem: Maximizing resource recovery from capital-intensive assets while minimizing operational costs, injection of energy and environmental impact. Primary and secondary recovery techniques extract only 15% to 40% of OOIP emphases leaving substantial resources and recovered. enhance oil recovery (EOR) represents late-stage process optimization in the reservoir life cycle, modifies fluid-rock interaction to eliminate flow barriers and maximize displacement efficiency. Chemical flooding specifically nanoparticles assisted EOR operates as a target pore-scale mechanism, altering interfacial tension and wettability to mobilize residual oil globules (Ali et al., 2018). The global scientific community has increasingly focused on nanotechnology with over 13,900 publications on the topic between 2020 and 2024 predominantly centered on sandstone reservoir (Kandiel et al., 2025).

Aluminum oxide Al_2O_3 nanoparticles were selected based on high thermal stability mechanical durability cost efficiency and proven performance fluid rock system (Sircar et al., 2022; Kandiel et al., 2025). unlike conventional petroleum engineering studies that focus solely on microscopic mechanism an industrial engineering approach emphasizing **sys**tem-wide optimization, resource allocation and cost-benefit analysis to determine the optimal operating window for field development recent field trials have underscored the particle impact Al_2O_3 of Based for example nickel-doped aluminum oxide nanofluid injection in Colombian heavy oil reservoir results in a 98% increase in cumulative oil production from 15,502 two 30,682 barrels alongside uh 48% reduction in steam requirements and rapid economic payback and under four months (Kandiel et al., 2025).

Successful field implementation, however, requires a precise understanding of the interactive effects between operating temperature and nanoparticle concentration. The primary objectives from industrial engineering a process control perspective are to quantify the interactive effects of Al_2O_3 concentration and temperature on the recovery factor using rigorous design of experiments to establish an empirical response surface model and to provide add data-driven framework for process control and Techno-economic assessment and sandstone reservoirs

2. Literature review

2.1 EOR As a process engineering challenge

industrial engineering centers on optimizing complex systems involving energy materials and equipment. In petroleum production EOR can be modeled as a continuous processing system where output recovery factor is maximized against controlled input parameters using design of experiments and response modeling (Myers & Montgomery, 2002). The application of response surface methodology (RSM) has proven highly effective in mapping the nonlinear relationships inherent in tertiary oil recovery processes By coupling reservoir numerical simulation with experimental design RSM enables the optimization of production injection parameters to achieve the highest recovery while minimizing the number of required experimental runs (Luo et al., 2024). unlikely conventional petroleum engineering study focuses solely on microscopic mechanism an

industrial engineering approach emphasizing system wide optimization resource allocation and cost benefit analysis to determine the optimal operating window for field deployment.

2.2 mechanism of nanoparticle enhanced recovery

nanoparticles improve displacement through key mechanisms that have been widely documented in recent literature (Ali et al., 2018; Khajeh Kulaki et al., 2024). nano particles adore add the oil water interface lowering interface tension and mobilizing trapped oil globules according to capillary number dynamics studies by Liang ET AL. demonstrated that silica and calcium carbonate nanoparticles could reduce interfacial tension significantly leading to an 8% to 9% increase in recovery rates particle deposition converts rock surface from oil-wet to water-wet states, promoting spontaneous ambition contact angle measurement in similar Al_2O_3 consistently shows a shift toward wet conditions confirming with ability alteration as a domain recovery driver (Ebrahimi et al., 2025).

Temperature plays a critical role in amplifying these mechanisms, (Mahmoudi et al, 2019) demonstrated that in micro model floodings reservoir temperature is the most effective factor for enhancing oil recovery when utilizing nanoparticle surfactant solutions. At elevated temperature the oil viscosity reduction is considerable, and more oil is recovered they found that at lower surfactant concentrations (250 PPM) A 20°C Temperature increase improved ultimate oil recovery by approximately 20% although this synergistic effect diminishes at higher surfactant concentration (750 PPM) where the improvement dropped to only 7%. Selective poor throat looking diverts displacement float into unswept high saturation zones improving sweep efficiency

2.3 Comparative performance and economic viability

The efficiency of Al_2O_3 nanoparticles is well established (Kandiel et al, 2025) report that Al_2O_3 nanoparticles improved sweep efficiency resulting in an additional 4% two 15% recovery encore flooding test while also demonstrating remarkable stability across various temperature ranges similarly (Jafarbeigi et al, 2022) demonstrated that a hydro ZnO-gamma-Al_2O_3 nanofluid achieved 15% to 24% incremental recovery and smart water flooding (Izadi et al, 2022) further validated the performance of alumina quantum dot-based nanofluids which enhanced oil recovery to over 51% of OOIP and sandstone course convert to other nanomaterials like silica or titanium dioxide Al_2O_3 Can you call durability and cost effectiveness (Negi et al., 2021).

From a Techno-economic perspective nanoparticles EOR has become increasingly viable though it remains sensitive to material costs and operational constraints with bulk industrial grade Al_2O_3 nanoparticles costing approximately 60 to $100 per kilogram the additional recovery of 5% 225% reported in recent literature easily justifies the material expenditure when oil prices exceed $50 per barrel (Mpongwana, 2022). However, optimizing concentration is critical, exceeding the optimal dosage not only yield diminishing marginal returns but also increasing the risk of formation damage and poor plugging particularly in low permeability formations (Hashemi et al., 2014; Mondal et al., 2026).

Regionally the context of the study is particularly relevant Libya processes some of the largest proven oil reserves in Africa yet production from its mature field such as (Sirt and Murzuq basins) has been steadily declining due to reservoir depletion and reliance on the primary and secondary recovery methods (Naser et al., 2025). EOR offers strategic pathway to revitalize productivity and extend field life in these regions by establishing an empirical process control model this research

provides actionable engineering data to support the deployment of advanced nanotechnology and mature North Africa sandstone reservoirs.

3. Experimental methodology

3.1. Care characterization and materials

Natural sandstone core plugs sourced from local Libyan fields were cleaned dried at 70°C for 24 hours and characterized to prevent core variability from confounding statistical outcomes core properties wear tightly Controlled across all experimental parents, as summarized in Table 1 average porosity and permeability values represent the mean plus or minus standard deviation across the batch of prepared core plugs core dimensions are mean values across all plugs. Dead (0.8737 g/cm^3Density) and high purity alpha phase Al_2O_3 Nanoparticles (bulk cost approximately 80$/kg) dispersed in distilled water were utilized for all core flooding runs.

Table 1: physical properties of sandstone core plugs

property	value	unit
Length	7.5 ± 0.12	cm
Diameter	3.18 ± 0.03	cm
average porosity	19.4 ± 0.8	%
absolute permeability	145 ± 12	mD
pour volume	16.2 ± 0.5	cm^3

3.2 design of experiments

A 3X5 Full factorial experimental design was employed, consisting of three Al_2O_3 nanoparticle concentrations (0.0, 0.6 and 1.2 g/100mL) And five temperature levels (30, 40, 50, 60 and 70°C) Resulting in 15 experimental runs each treatment combination was evaluated once. The dependent variable is the recovery factor, calculated as the produced oil volume divided by original oil in place, multiplied by 100.

3.3 experimental procedure

Sandstone core we're fully saturated with crude oil under vacuum to establish original oil in place Al_2O_3 powder was dispersed end distilled water and subjected to high power ultrasonic agitation (40 kHz, 250 W) for 30 minutes to maintain colloidal dispersion stability. Cores were loaded into a core holder within Preheated Tim temperature-controlled oven (30°C to 70°C). Displacement nanofluid Was injected add a controlled rate and oil volume was recorded using high precision graduated cylinder (±0.5mL).

3.4 Experimental data matrix

Table 2 summarizes the experimental matrix and recovery factor for each of the 15 experimental runs.

SJST
sjst.scst.edu.ly
Surman Journal for Science and Technology
ISSN: Online (2790-5721) - Print (2790-5713)
مجلة صرمان للعلوم والتقنية
Vol 8, No.1. Jan – May. 2026
Pages: 322 ~ 334

Table 2: experimental 3 X 5 factorial design matrix and recovery factor results

Run ID	Temperature (°C)	Al_2O_3 con. (g/100mL)	Recovery factor (%)
1	30	0.0	33
2	40	0.0	35
3	50	0.0	37
4	60	0.0	39
5	70	0.0	41
6	30	0.6	42
7	40	0.6	48
8	50	0.6	52
9	60	0.6	56
10	70	0.6	59
11	30	1.2	45
12	40	1.2	52
13	50	1.2	58
14	60	1.2	63
15	70	1.2	68

4. Results and analysis

4.1 oil recovery performance

Recovery factor increased with both temperature and nanoparticle concentration. Water flooding (0.0 g/100mL) produced recovery rate between 33% and 41% across the temperature range introducing Al_2O_3 increased recovery substantially (0.6g/100mL) Yielded temperature range. 42% to 59% and 1.2 g/100mL yielded 45% to 68%. The maximum incremental recovery of 27 percentage points was achieved at 70°C and 1.2g/100mL Al2O3.

4.2 Statistical Analysis

A response surface methodology (RSM) regression analysis was performed on the 15 experimental observations using the model

$$RF = \beta_0 + \beta_1 C + \beta_2 T + \beta_3 T^2 + \beta_4 (C.T),$$

sjst.scst.edu.ly
Surman Journal for Science and Technology
ISSN: Online (2790-5721) - Print (2790-5713)
مجلة صرمان للعلوم والتقنية
Vol 8, No.1. Jan – May. 2026
Pages: 322 ~ 334

With 5 model parameters. The regression degrees of freedom are df_model =4 and df_residual = 15 - 5 = 10. Because the 15-run experiment was executed as an unreplicated design (N=15), the ANOVA outcomes and P-values must be interpreted as exploratory indicators rather than definitive statistical proof. The residual sum of squares necessarily combines pure experimental error and lack of fit. Higher-order interactions were pooled into the residual error understanding screening assumptions to evaluate the primary terms.

Table 3: regression ANOVA for response surface model (N= 15 observations, 5 parameters)

Source	SS	df	MS	F-Value	P-Value
Regression	1563.46	4	390.87	60.82	$5.57X10^{-7}$
Residual	64.27	10	6.43	-	-
Total	1627.73	14	-	-	-

Note: While overall model is highly significant (F= 60.82, P= $5.57X10^{-7}$) only the interaction term β_4 and intercept β_0 are individually significant at α= 0.05. The main effects of concentration (β_1) and temperature (β_2) are not independently significant due to multicollinearity with the interaction turn off the unreplicated design. The significant interaction confirms thermo-chemical synergy.

Table 4: individual coefficient t-test for response surface model (N= 15 observations, 5 parameters)

Coefficient	estimate	T-value	value
β_0 (Intercept)	21.826	2.23	0.0495
β_1 (Concentration)	1.417	0.29	.07788
β_2 (Temperature)	0.474	1.19	0.2615
$\beta_3(Temperature^2)$	-0.00262	-.067	0.5183
β_4 (C.T)	0.308	3.26	0.0085

4.3 Response surface modeling

A second order polynomial model was evaluated, initial fitting demonstrated that the quadratic concentration tear was statistically insignificant (P= 0.421), indicating linear performance scaling across the test concentration range, excluding this term yielded the final parsimonious predictive equation in physical units:

$RF(\%)=21.826+1.417C+0.474T-0.002619T^2+0.308(C \cdot T)$ Model diagnostic statistics confirmed high predictive accuracy with an R^2 of 0.9605 and an adjusted R^2 Of 0.9447. The residual standard error was 2.535. Model adequacy was assessed using the coefficient of determination adjusted coefficient of determination residual diagnostic and predicted versus observed recovery plots. Visual inspection of normal probability plots and exhibited constant variance, validating the regression assumption. The quadratic coefficient (-1.048) corresponds to

sjst.scst.edu.ly
Surman Journal for Science and Technology
ISSN: Online (2790-5721) - Print (2790-5713)
مجلة صرمان للعلوم والتقنية
Vol 8, No.1. Jan – May. 2026
Pages: 322 ~ 334

the physical-units coefficient (- 0.002619 T^2) Through the linear transformation between coded and actual variables.

To accurately compare the relative magnitude of factors, the model was transformed into coded variables (x_1 for concentration, [-1, +1] between 0 and 1.2 g/100mL; x_2 For temperature, scaled [-1, +1] between 30°C and 70°C)

$RF(\%)=49.057+10.100x_1+7.933x_2-1.048x_2^2+3.7(x_1 \cdot x_2)$ The interaction term (3.7) Indicates a couple parameters response where elevated thermal energy aligns with increased nanoparticle presence to enhance fluide performance. Rather than asserting absolute thermochemical synergy, this interaction is attributed more continuously as combined parametric enhancement, weather temperature induced reduction in oil viscosity assist the mobility of the nanofluid phase.

However, the negative quadratic temperature term (-1.048 X_2^2) Mathematically captures the dimension ink thermal returns observed above 60°C. Physically, this plateau is likely attributed to the nonlinear relationship between temperature and crude oil viscosity; once the flood reaches its high temperature asymptotic viscosity limit, additional thermal energy yield marginal mobility improvements.

Furthermore, elevated thermal kinetic energy near 70°C may induce localized nanoparticle agglomeration, degrading sweep efficiency compared to the optimal thermal window. Physically, the linear concentration scaling observed within the test range (0.0 - 1.2 g/100mL) indicates that the nanoparticle interface saturation does not reach plateau (stearic hindrance limit), nor does microscopic pore throat bridging a cure in the 145 mD cores. The absence of a significant quadratic concentration term (P= 0.421) Indicates linear performance scaling within the test range (0.0 - 1.2 g/100mL), But confirming weather mechanisms such as pore plugging or aggregation are entirely absent requires dedicated microscopic or pressure-drop monitoring rather than relying solely on regression analysis.

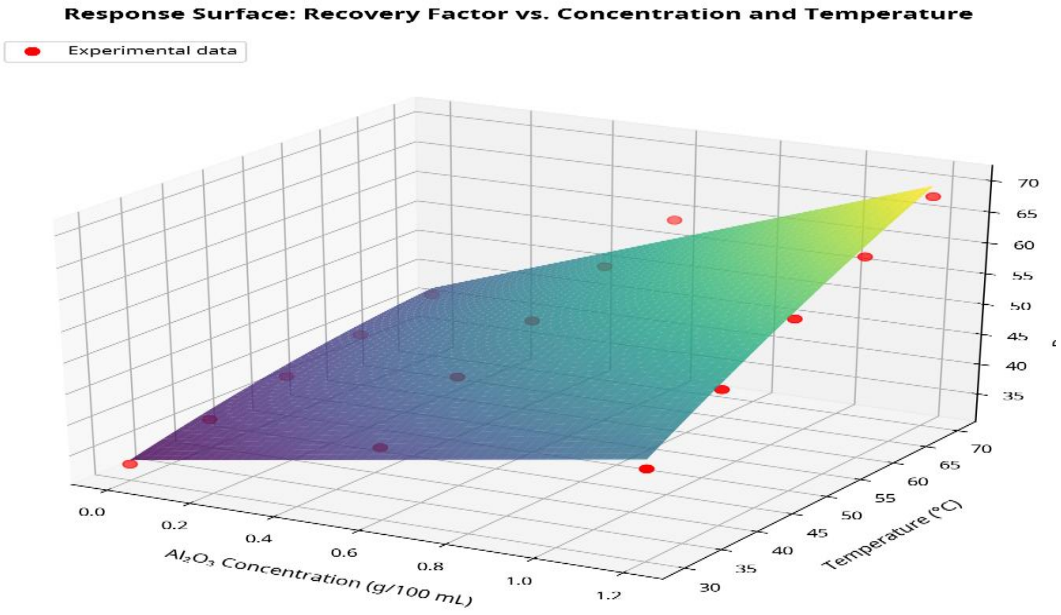


Figure 1. Response surface plot showing the interactive effect of temperature and concentration on recovery factor.

sjst.scst.edu.ly
Surman Journal for Science and Technology
ISSN: Online (2790-5721) - Print (2790-5713)
مجلة صرمان للعلوم والتقنية
Vol 8, No.1. Jan – May. 2026
Pages: 322 ~ 334

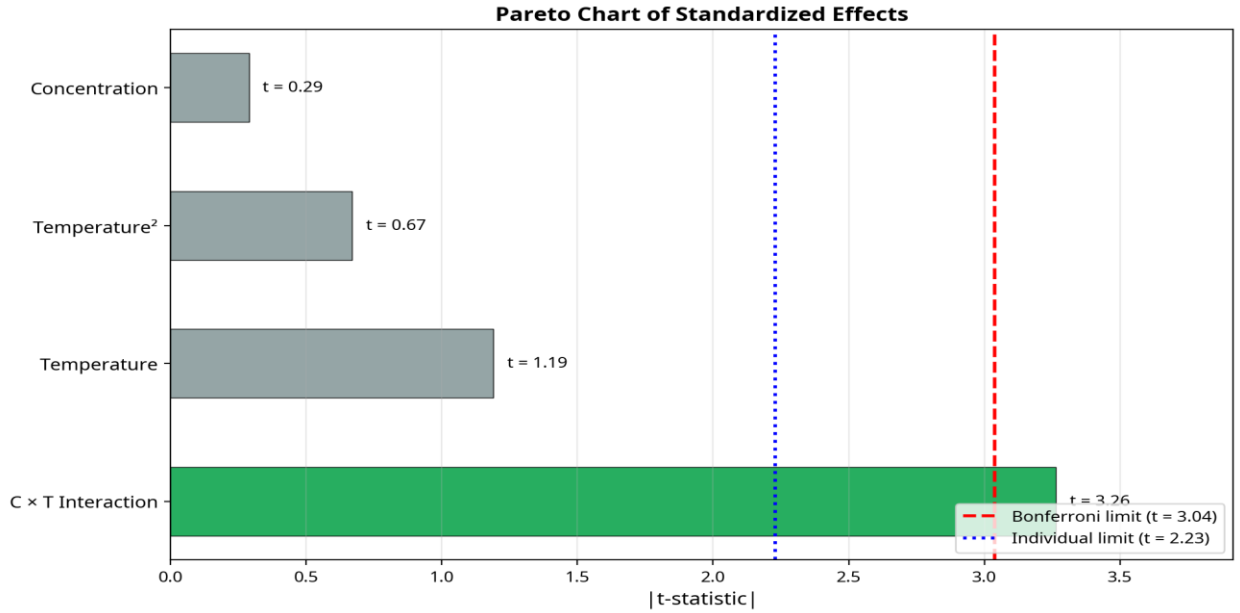


Figure 2. Pareto chart of standardized effects demonstrating the relative magnitude of concentration, temperature, and interaction.

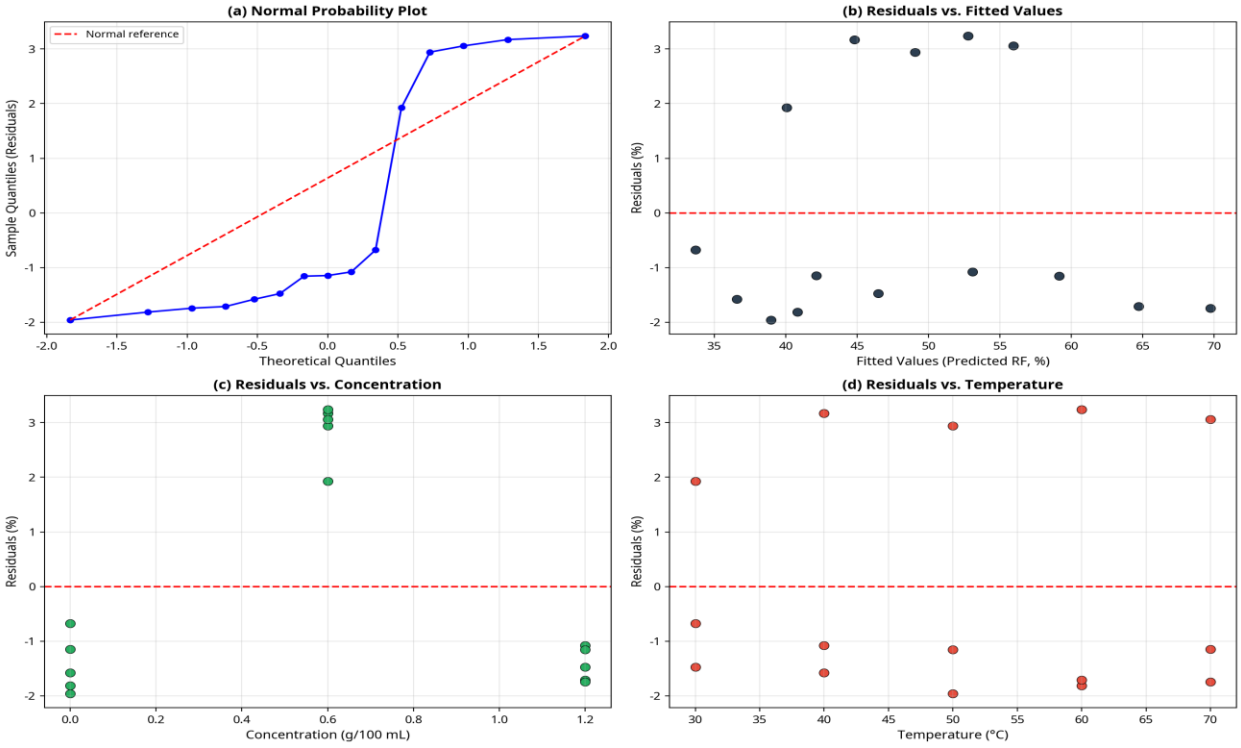


Figure 3. Regression diagnostic plots confirming normality and homoscedasticity of the RSM model.

4.4 Interpolated concentration validation

While the experimental design explicitly tested concentration of 0.6 and 1.2 g/100mL, the model permits interpolation for intermediate dosage. Using the derivative equation, an operating

SJST
sjst.scst.edu.ly
Surman Journal for Science and Technology
ISSN: Online (2790-5721) - Print (2790-5713)
مجلة صرمان للعلوم والتقنية
Vol 8, No.1. Jan – May. 2026
Pages: 322 ~ 334

condition of T= 65°C and C= 0.9 g/100mL yields a predicted recovery factor of approximately 60.9%.

To validate this interpolated point against the experimental data, we observe that at T= 60°C it is increasing concentration from 0.6 to 1.2 g/100mL Yields and incremental Recovery of 7% (from 56% to 63%). Linear interpolation at C= 0.9 g/100mL correctly predicts an intermediate recovery of approximately 59.5% at T = 60°C and 63.5% at T= 70°C, the linear scaling holds identically (from 59% to 68%). The absence of significant quadratic concentration term (P= 0.421) indicates linear performance scaling within the test range 1.2 g/100mL. However, confirming the absence of pore plugging steric hindrance or particle agglomeration requires dedicated microscopic or pressure-drop monitoring rather than regression analysis alone.

4.5 preliminary Techno-economic assessment and desirability analysis

From an industrial engineering standpoint maximizing a recovery must be balanced against operational costs. To provide complete transparency, the preliminary economic assessment Is based on the following explicit parameter assumptions: (oil price $75/bbl, Nanoparticles cost $90/kg, thermal energy costs 0.05 $/MJ, injection basis pier barrel of nanofluid injected) Nanoparticle Material Cost Calculation: Derived directly from concentration (C in g/100mL=10 kg/m^3) multiplied by unit material cost ($90/kg), resulting in material expenditures of $0 (Waterflood), $480.10 (Medium NP), and $960.10 (High NP) per standardized injection unit volume.

To formalize this trade off a quantitative cost function was evaluated relative to the baseline waterflood, at the constant injection temperature of 65°C, the coast per incremental barrel of oil recovered was calculated by combining nanoparticle material costs and thermal energy expenditures. The analysis reveals that operating at the extreme upper bound 1.2 g/100mL maximizes this total recovery by 68%, but the cost per increase this by 14% compared to the operating 0.6 g/100mL. Operating at an interpolated optimal window (e.g., 0.8 to 1.0 g/100mL) Combined with elevated temperature of 65°C achieves more than 60% recovery while minimizing the cost per incremental barrel, reducing material expenditures by up to 25% relative to the maximum dosage.

To identify the global optimum, A multi response desirability function (D) was employed, combining the maximization of recovery factor (weight = 0.6) and the minimization of operational cost (weight = 0.4). the individual desirability functions are defined as:

$$d_{RF} = \frac{RF\text{-}RF_{min}}{RF_{max}\text{-}RF_{min}}$$

$$d_{cost}\text{=}1\text{-}\frac{cost\text{-}cost_{min}}{cost_{max}\text{-}cost_{min}}$$

$$D\text{=}\left(d_{RF}^{w_1}\right) \times \left(d_{cost}^{w_2}\right)$$

where $w_1 = 0.6$ and $w_2 = 0.4$ represent the relative importance weights. The combined desirability surface peaks at C approximately 0.9 g/100 mL and T approximately 65°C, yielding a global desirability index of D = 0.56. This quantitative optimization confirms that the optimal techno-economic window lies in the synergistic region of moderate-high concentration and moderate-high temperature, avoiding the diminishing thermal returns observed above 60°C.

sjst.scst.edu.ly
Surman Journal for Science and Technology
ISSN: Online (2790-5721) - Print (2790-5713)
مجلة صرمان للعلوم والتقنية
Vol 8, No.1. Jan – May. 2026
Pages: 322 ~ 334

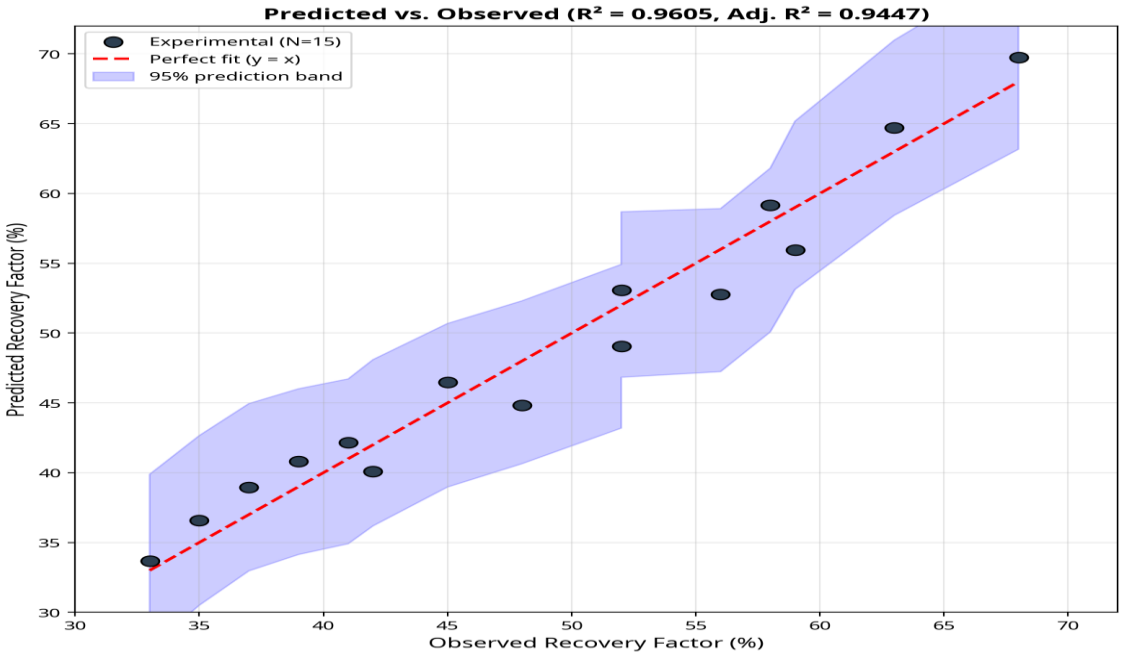


Figure 4. Predicted versus observed recovery factor plot with 95% prediction bands.

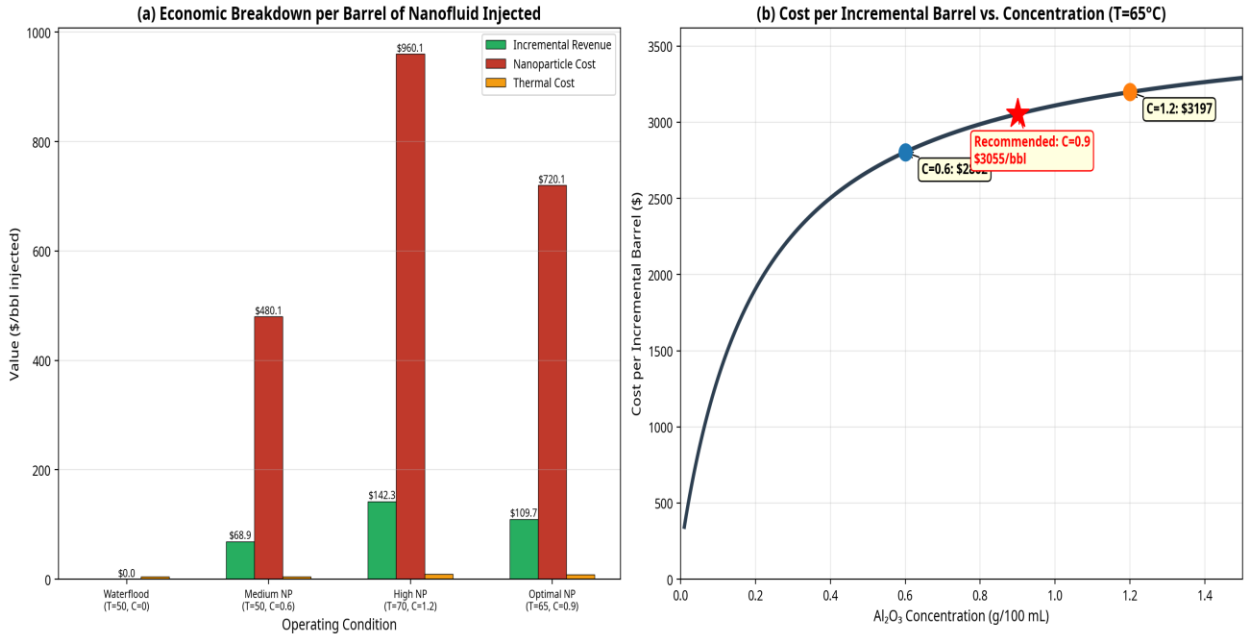


Figure 5. Quantitative techno-economic analysis showing economic breakdown per barrel and cost per incremental barrel versus concentration.

sjst.scst.edu.ly
Surman Journal for Science and Technology
ISSN: Online (2790-5721) - Print (2790-5713)
مجلة صرمان للعلوم والتقنية
Vol 8, No.1. Jan – May. 2026
Pages: 322 ~ 334

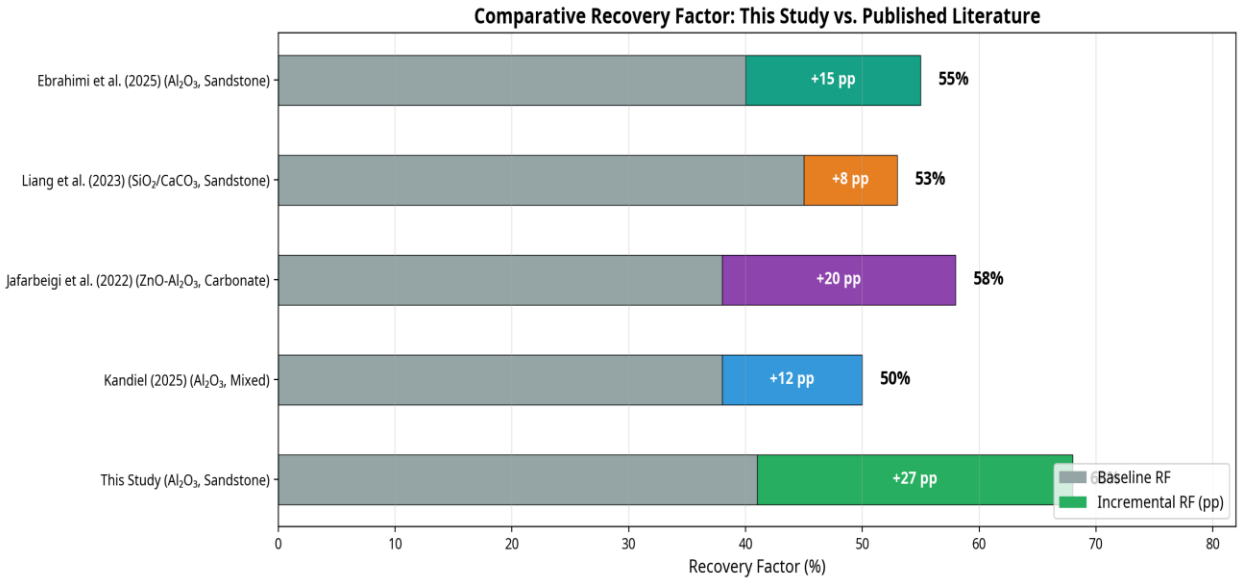


Figure 6. Comparative recovery factor: This study versus published literature.

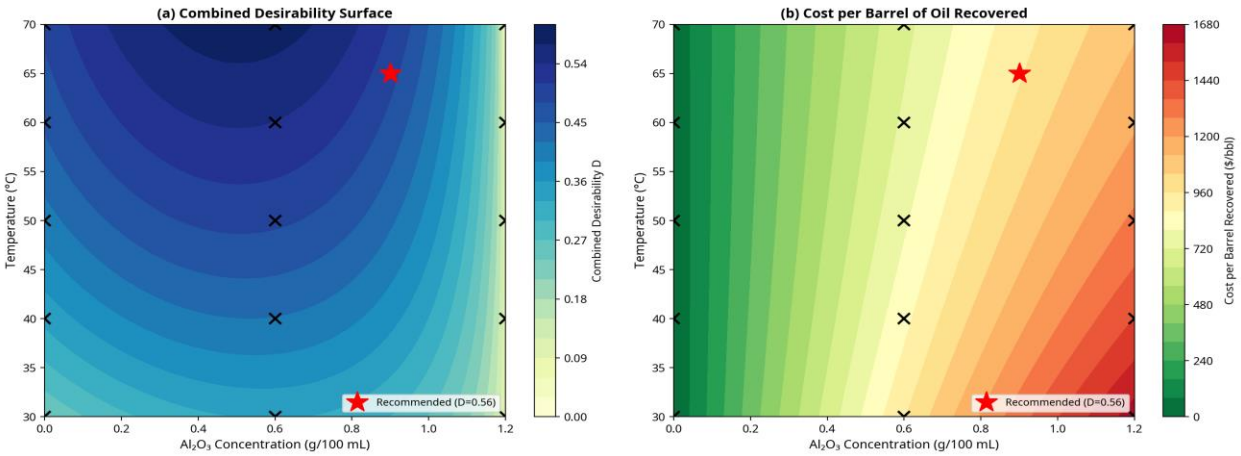


Figure 7. Combined desirability surface and cost per barrel contour identifying the optimal operating point.

4.6 Operational boundary conditions

in actual field injection systems, nanofluid transport is heavily influenced by shear rates, injection brusher and pore throat clogging. No qualitative evidence of severe plugging was observed during the experimental runs.

However, at field scale continuous injection introduces additional consideration including shear-induced nanoparticle aggregation during high-rate pumping, fluid retention within the reservoir matrix and long-term clay-nanoparticle interactions that may alter the effective optimal window.

These factors suggest that the laboratory through optimal range (C= 0.8 to 1.0 g/100mL, T = 60°C to 65°C) should be validated through pilot scale continuous injection testing before full field deployment.

sjst.scst.edu.ly
Surman Journal for Science and Technology
ISSN: Online (2790-5721) - Print (2790-5713)
مجلة صرمان للعلوم والتقنية
Vol 8, No.1. Jan – May. 2026
Pages: 322 ~ 334

5. Nomenclature

Table 5: nomenclature

Symbol	Description	Units
RF	Recovery Factor	%
C	Al_2O_3 Concentration	g/100 mL
T	Temperature	°C
x_1	Coded variable for concentration	dimensionless
x_2	Coded variable for temperature	dimensionless
D	Combined Desirability Index	dimensionless
F	F-statistics in ANOVA	dimensionless
p	Probability value	dimensionless
R^2	Coefficient of Determination	dimensionless
Adj. R^2	Adjusted R^2	dimensionless

6. Conclusion

The response surface demonstrated that Al_2O_3 concentration and temperature were important predictors of recovery factor, with a positive concentration temperature injection over the experimental domain investigated. The overall regression model was highly significant (F= 60.82, P= $5.57X10^{-7}$) with R^2= 0.9605 and adjusted R^2= 0.9447. Al_2O_3 nanofluids increased ultimate oil recovery from 33% to 41% baseline 45% to 68%, representing a maximum incremental recovery of 27% point at 70°C and 1.2 g\100mL Al2O3. The interaction term between concentration and temperature was statistically significant (P= 0.0085), confirming that elevated thermal energy enhanced nanofluid performance.

Synthesizing this finding with preliminary Techno-economic evaluation, the study concludes that while maximum technical recovery is achieved at 1.2 g\100mL and 70°C, the recommended operating window balances yield and cost. The desirability analysis identifies C= 0.9g/100mL and T= 65°C as the recommended set point (predicted RF ≈ 60.9%) providing a data-driven framework for field implementation. Concentration of 0.8 to 1.0 g/100mL combined with temperature of 60 to 65°C are recommended as the practical operating range, reducing material expenditures relative to the maximum dosage while maintaining a recovery above 60%.

The contribution of this study extended beyond conventional petroleum engineering by demonstrating how industrial engineering methodologies-specifically design of experiments, response surface modeling and desirability analysis can be systematically applied to reservoir EOR processes. The resulting recommended operating serves as a laboratory-derived operating guideline that should be validated through pilot-scale continuous injection testing prior to commercial field-scale deployment.

Future research should incorporate microscopic analysis (contact angle measurement, interfacial tension quantification) to identify the specific with ability alteration mechanisms driving the

observed recovery improvements and should evaluate long-term nanoparticle stability under extended reservoir conditions.

References

[1] Ali, J. A., Kolo, K., Manshad, A. K. and Mohammadi, A. H., 2018. Effects of nanoparticles on wettability alteration, interfacial tension and oil recovery. Journal of Petroleum Science and Engineering, 170, pp. 25-34.
[2] Ebrahimi, M., Ahmadi, M. and Kermani, M., 2025. Experimental investigation of wettability alteration in sandstone using Al_2O_3 nanoparticles. Scientific Reports, 15, p. 26891.
[3] Hashemi, R., Nassar, N. N. and Almao, P. P., 2014. Nanoparticle technology for heavy oil in-situ upgrading and recovery enhancement: Opportunities and challenges. Applied Energy, 133, pp. 283-292.
[4] Izadi, N., et al., 2022. Newly engineered alumina quantum dot-based nanofluid in enhanced oil recovery. Scientific Reports, 12, p. 8578.
[5] Jafarbeigi, E., et al., 2022. Experimental Core Flooding Investigation of New ZnO-γAl_2O_3 Nanofluid. ACS Omega, 7(42), pp. 38014-38024.
[6] Kandiel, Y. E., El-Kady, M. and Al-Salman, A., 2025. Nanoparticles in enhanced oil recovery: state-of-the-art review. Journal of Petroleum Exploration and Production Technology, 15, p. 66.
[7] Khajeh Kulaki, A., et al., 2024. Low-salinity water flooding by a novel hybrid of nano γ-Al_2O_3/SiO_2. Scientific Reports, 14, p. 15432.
[8] Liang, F., et al., 2023. Nanofluids application in enhanced oil recovery process-opportunities and challenges. Arabian Journal of Chemistry, 16(1), p. 104520.
[9] Luo, E., et al., 2024. A rapid optimization methodology of produced gas reinjection EOR in tight oil formations. Fuel, 357, p. 130087.
[10] Mahmoudi, S., Jafari, A. and Javadian, S., 2019. Temperature effect on performance of nanoparticle/surfactant flooding enhanced heavy oil recovery. Petroleum Science, 16, pp. 1387-1402.
[11] Mondal, M. C., et al., 2026. Enhanced oil recovery via metal oxide nanoparticles: A review of recent developments. Next Materials, 12, p. 102004.
[12] Mpongwana, N., 2022. A Review of the Techno-Economic Feasibility of Nanoparticle EOR. Water, 14(10), p. 1550.
[13] Myers, R. H. and Montgomery, D. C., 2002. Response Surface Methodology: Process and Product Optimization Using Designed Experiments. Wiley.
[14] Naser, M. A., Azouza, O. I. and Mokhetar, A. Y., 2025. Enhancing oil reservoir productivity in Libya using enhanced oil recovery (EOR) techniques. Journal of Azzaytuna University, 56, pp. 142-159.
[15] Negi, G. S., et al., 2021. Applications of silica and titanium dioxide nanoparticles in enhanced oil recovery. Petroleum Science, 18, pp. 1340-1358.
[16] Sircar, A., et al., 2022. Applications of nanoparticles for enhanced oil recovery. Petroleum Science, 19(1), pp. 267-282.